J|A|C|S
ARTICLES
Published on Web 08/10/2006

Small Polaron Hopping in Li_xFePO_4 Solid Solutions: Coupled Lithium-Ion and Electron Mobility

Brian Ellis,[†] Laura K. Perry,[‡] Dominic H. Ryan,[‡] and L. F. Nazar*,[†]

Contribution from the Department of Chemistry, University of Waterloo, 200 University Avenue West, Waterloo, Ontario, Canada N2L 3G1, and Department of Physics, McGill University, 3600 University Street, Montreal, Quebec, Canada H3A 2T8

Received February 28, 2006; E-mail: lfnazar@uwaterloo.ca

Abstract: Transition metal phosphates such as $LiFePO_4$ have been recognized as very promising electrodes for lithium-ion batteries because of their energy storage capacity combined with electrochemical and thermal stability. A key issue in these materials is to unravel the factors governing electron and ion transport within the lattice. Lithium extraction from $LiFePO_4$ results in a two-phase mixture with $FePO_4$ that limits the power characteristics owing to the low mobility of the phase boundary. This boundary is a consequence of low solubility of the parent phases, and its mobility is impeded by slow migration of the charge carriers. In principle, these limitations could be diminished in a solid solution, Li_xFePO_4. Here, we show that electron delocalization in the solid solution phases formed at elevated temperature is due to rapid small polaron hopping and is unrelated to consideration of the band gap. We give the first experimental evidence for a strong correlation between electron and lithium delocalization events that suggests they are coupled. Furthermore, the exquisite frequency sensitivity of Mössbauer measurements provides direct insight into the electron hopping rate.

Introduction

The $LiMPO_4$ family adopts a common structure displayed by silicate minerals such as olivine, $MgFeSiO_4$, that constitute a large fraction of the earth's crust. The lattice comprises a network of MO_6^{n+} octahedra (M = metal) interwoven with XO_4^{n-} tetahedra (X = Si, P). The mobile alkali ions, Li^+ in the case of $LiMPO_4$ (M = Fe, Ni, Co, Mn), form one-dimensional chains in the structure that run parallel to planes of corner-shared MO_6 octahedra, and along the [010] direction in the orthorhombic *Pnma* lattice. The iron phase was first proposed as a cathode material in lithium-ion batteries almost a decade ago[1] and has shown considerable promise due to its excellent cyclability, stability, and low cost. Much recent effort has been focused on creating olivine phases with better conductivities. Transport of lithium ions and electrons within the lattice is still poorly understood and is the subject of some recent debate. The lithium ion mobility along the chain direction is predicted to be relatively facile based on calculations of "free" ion transport (i.e., in the absence of interactions with the framework, and localized electron sites),[2] but other reports suggest that the material is a slow ion conductor.[3] With respect to electron mobility, the electronically insulating effect of the tetrahedral PO_4^{3-} groups on which the inductive effect relies unquestionably gives rise to isolation of the redox centers within the lattice. The controversy regarding the source of the low electronic conductivity in $LiMPO_4$ phases suggests the underlying principles remain clouded, however. Many reports have claimed the electronic conductivity in $LiFePO_4$ is correlated to the band gap—the estimates of which vary widely from no gap at all, to a small gap based on band structure calculations.[4−8] More sophisticated calculations that include correlation effects indicate it is much higher[9] and are confirmed by optical measurements that place it at about 3.7 eV.[9] Electron transport in such poor semiconductors typically takes place by small polaron migration, generated by either hole or electron carriers.[10] Here as well, experimental values for the activation energy vary greatly. Values of 630 meV and 390−500 meV have been determined using ac conductivity[11] and dc conductivity, respectively.[8] Substantially lower estimates of 155 meV have also been reported based on ac impedance spectroscopy,[12] and 186 meV based on dc conductivity measurements on Cr-doped materials.[7] Values for *unconstrained* polaron transport derived

† University of Waterloo.
‡ McGill University.

(1) Padhi, A. K.; Nanjundaswamy, K. S.; Goodenough, J. B. *J. Electrochem. Soc.* **1997**, *144*, 1188.
(2) Morgan, D.; Van der Ven, A.; Ceder, G. *Electrochem. Solid-State Lett.* **2004**, *7*, A30.
(3) Whittingham, M. S.; Song, Y.; Lutta, S.; Zavalij, P. Y.; Chernova, N. A. *J. Mater. Chem.* **2005**, *15*, 3362.
(4) Yamada, A.; Chung, S.-C. *J. Electrochem. Soc.* **2001**, *148*, A960.
(5) Yamada, A.; et al. *J. Power Sources* **2003**, *119*, 232.
(6) Tang, P.; Holzwarth, A. W. *Phys. Rev. B: Condens. Matter Mater. Phys.* **2003**, *68*, 165107.
(7) Shi, S. Q.; Liu, L. J.; Ouyang, C.; Wang, D. S.; Wang, Z. X.; Chen, L. Q.; Huang, X. J. *Phys. Rev B: Condens. Matter Mater. Phys.* **2003**, *68*, 195108.
(8) Xu, Y. N.; Chung, S.-Y.; Bloking, J. T.; Chiang, Y. M.; Ching, W. Y. *Electrochem. Solid-State Lett.* **2004**, *7*, A131.
(9) Zhou, F.; Kang, K.; Maxisch, T.; Ceder, G.; Morgan, D. *Solid State Comm.* **2004**, *132*, 181.
(10) Rosso, K.; Smith, D. M. A.; Dupuis, M. *J. Chem. Phys.* **2003**, *118*, 6455.
(11) Delacourt, C.; Laffont, L.; Bouchet, L.; Wurm, C.; Leriche, J.-B.; Tarascon, J.-M.; Masquelier, C. *J. Electrochem. Soc.* **2005**, *152*, A913.
(12) Takahashi, M.; Tobishima, S.; Takei, K.; Sakurai, Y. *Solid State Ionics* **2002**, *148*, 283.

10.1021/ja0614114 CCC: $33.50

Scheme 1. Illustration of the Two-Phase Mixture of Triphylite ($LiFePO_4$) and Heterosite ($FePO_4$) Formed on Extraction of Li from $LiFePO_4$ at Room Temperature, and the Movement of the Phase Boundary[a]

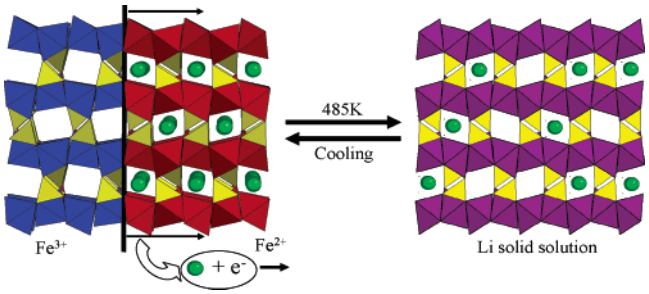

[a] Upon heating the composite to 485 K, a solid solution Li_xFePO_4 forms. On cooling, the parent phases recrystallize, and nucleation and growth take place everywhere within the crystal (not depicted for simplicity).

from first principles calculations are in the range of 185−220 meV, but this model assumes no interaction of the polarons with the lattice. The actual activation energy for hopping is predicted to be much higher in the presence of strong binding to the lithium ion.[13]

When lithium is partially extracted from the structure, formation of a $LiMPO_4/MPO_4$ mixture is in part driven by the 6% volume change between the phases. This is illustrated in Scheme 1 for the triphylite/heterosite composite that characterizes $Li_{1-x}FePO_4$. The solubility of the two phases at room temperature is not accurately known. Some reports suggest a pure two-phase coexistence with no mutual solubility,[14] whereas others give evidence for very narrow single-phase regimes $Li_\alpha FePO_4$ and $Li_{1-\beta}FePO_4$.[15,16] Very recently, neutron diffraction data have been reported that claim a somewhat wider region of solid solution at room temperature, with α and $1-\beta$ of 0.05 and 0.89, respectively.[17] In the absence of any solid solution domains, of course, lithium ion extraction and Li^+ ion transport within the pure parent members are difficult to explain. Nonetheless, the very limited solubility is probably responsible for the electrochemical limitations of the material owing to the low intrinsic ionic and electronic conductivity and, hence, low mobility of the phase boundary. However, at elevated temperatures, the solubility increases to 100%: it was recently shown that a transition to a Li_xFePO_4 ($0 < x < 1$) solid solution (SS) phase occurs at about or above 485 K.[18] This is a SS with respect to lithium concentration, where lithium occupation is random within the lattice. We wanted to determine the onset temperature of *electron* delocalization and see if this was correlated to the state of lithium disorder. The discrepancy between calculated (predicted) estimates for isolated carrier transport activation energies and values measured experimentally also suggests that the lithium mobility is affected by the electron mobility via strong interactions (and vice versa): a point we wished to explore further here. To our knowledge, no study of this nature on the atomic scale in Li_xFePO_4 or other phosphates is available thus far. The coupled mobility of Li^+ and e^-, although an intriguing concept, has not been demonstrated. Reports have correlated ionic and electronic hopping in oxides, namely $LiMn_2O_4$[19] and Li_xNiO_2,[20] on the basis of molecular dynamics and solid state NMR studies, respectively. Nonetheless, as stated by others, much work is still needed for fully understanding the nature of charge carriers in $LiMPO_4$-type materials.[15,18] Such knowledge would give insight into the transport mechanism not only in $LiFePO_4$, but in an ever increasing family of phosphate, fluorophosphate, and silicate materials being considered as the new generation of lithium-ion cathodes.

The substantial increases in both isomer shift and quadrupole splitting observed in a Mössbauer spectrum on going from Fe^{3+} to Fe^{2+}, coupled with the phase-quantitative nature of the measurement, makes Mössbauer spectroscopy an ideal technique for this study. More importantly, Mössbauer is also sensitive to dynamics on time scales comparable to the precession time of the ^{57}Fe nucleus in the magnetic field or electric field gradient (efg) to which it is exposed.[21] In a magnetic field, this time is usually denoted τ_L, the Larmor precession time; however, no standard term exists for the quadrupolar precession that occurs in an efg, so we denote it τ_Q. In a simple two-level model, the hyperfine environment of the ^{57}Fe nucleus fluctuates between two distinct states (Fe^{2+} and Fe^{3+} here). If the time scale of this relaxation, τ_R, is much longer than τ_Q, then two static patterns, one corresponding to each of the two environments, are observed. At the other extreme, where τ_R is much shorter than τ_Q, the ^{57}Fe nucleus experiences an averaged environment and a single "motionally narrowed" component is observed in the spectrum. For intermediate relaxation times, the spectra are more complex, showing broadened lines and greatly modified spectral line shapes. In the materials studied here, τ_Q is about 3×10^{-8} s (the observed quadrupole splitting in the Fe^{2+} component is ~3 mm/s) so motional narrowing sets in for $\tau_R \leq \tau_Q$ and the "Mössbauer window" is open from about 10^{-10} s (beyond which dynamic effects are too fast to be observed and a "static" averaged pattern is measured) to about 10^{-6} s (where the two spectral components are each effectively static). Quantitative information on dynamics can only be obtained within this window. Relaxation rates increase with temperature, and this temperature dependence can be used to determine the activation energy for the relaxation process. Thus, Mössbauer spectroscopy will allow us to measure both the small polaron hop rate and its activation energy, as we demonstrate below.

Experimental Section

Preparation of Li_xFePO_4. Three samples were prepared: $Li_{0.75}FePO_4$ made by the sol−gel method,[18] $Li_{0.55}FePO_4$ made by sol−gel method,[18] and $Li_{0.25}FePO_4$ made by the iron oxalate method.[8] Solid solutions (with respect to lithium content) of $Li_{1-x}FePO_4$ were prepared by partial oxidation of $LiFePO_4$ by treatment with $NOBF_4$ in solution to three targeted stoichiometries: $Li_{0.25}FePO_4$, $Li_{0.55}FePO_4$, and $Li_{0.75}FePO_4$. Partial oxidation resulted in intimate two-phase mixtures of $LiFePO_4/FePO_4$.

Mössbauer. Mössbauer spectra were collected using a 50mCi ^{57}Co**Rh** source mounted on a constant-acceleration spectrometer calibrated using α-Fe foil at room temperature. Approximately 25 mg

(13) Maxisch, T.; Zhou, F.; Ceder, G. *Phys Rev. B: Condens. Matter Mater. Phys.* **2006**, *73*, 104301.
(14) Yamada, A.; Kudo, Y.; Liu, K.-Y. *J. Electrochem. Soc.* **2001**, *148*, A1153.
(15) Srinivasan, V.; Newman, J. *J. Electrochem. Soc.* **2004**, *151*, A1517.
(16) Yamada, A.; Koizumi, H.; Sonoyama, N.; Kanno, R. *Electrochem. Solid-State Lett.* **2005**, *8*, A409.
(17) Yamada, A.; Koizumi, H.; Nishimura, S.-I.; Sonoyama, N.; Kanno, R.; Yonemura, M.; Nakamura T.; Kobayashi, Y. *Nature Mater.* **2006**, *5*, 357.
(18) Delacourt, C., Poizot, P.; Tarascon, J.-M.; Masquelier, C. *Nat. Mater.* **2005**, *4*, 254.
(19) Tateishi, K., du Boulay, D.; Ishizawa, N. *Appl. Phys. Lett.* **2004**, *26*, 529.
(20) Chazel, C.; Menetrier, M.; Croguennec, L.; Delmas, C. *Inorg. Chem.* **2006**, *45*, 1184.
(21) Dattagupta, S. In *Mossbauer Spectroscopy*; Dickson, D. P. E., Berry, F. J., Eds.; Cambridge University Press: Cambridge, 1986; p 198.

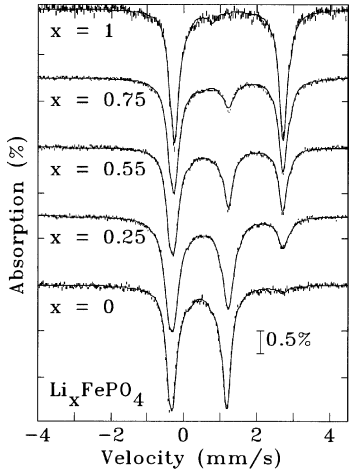

Figure 1. Room-temperature Mössbauer spectra of the compositions $LiFePO_4$, $Li_{0.75}FePO_4$, $Li_{0.55}FePO_4$, $Li_{0.25}FePO_4$, and $FePO_4$ showing the contributions of the localized Fe^{2+} and Fe^{3+} components in the two-phase mixtures. (See text for a discussion of the impurity phases).

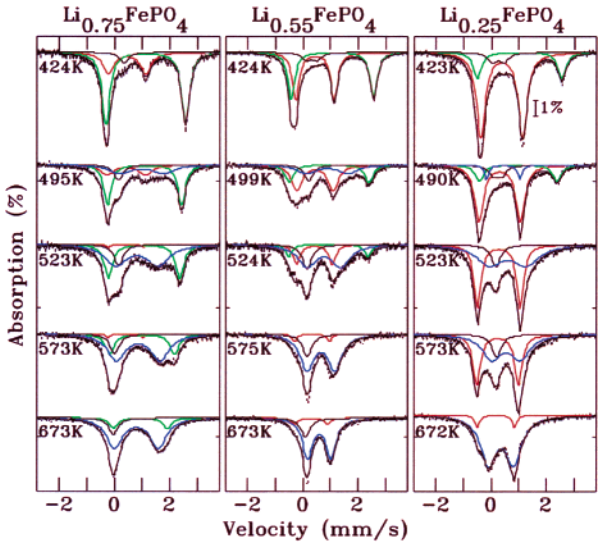

Figure 2. Mössbauer spectra recorded at elevated temperatures (indicated) illustrating the evolution from the two-phase composition to the solid solutions $Li_xFe^{2+/3+}PO_4$ as a function of temperature. Solid lines through the data are fits as described in the text. Additional solid lines show the contributions from the primary Fe^{2+} and Fe^{3+} components and, above 500 K, the broad solid solution phase.

of sample was mixed with BN powder and mounted in an evacuated furnace fitted with Be windows. The sample temperature was monitored using a type-K thermocouple, and temperature stability was better than 2 K for all measurements. Spectra were fitted to a sum of Lorentzian lines using a conventional nonlinear least-squares minimization routine. Each component was fitted with an independent line width to accommodate possible differences in disorder within each phase, and especially to allow for the dynamic broadening of the solid solution phase. All spectra were measured in an increasing temperature sequence. The sample was equilibrated for 3 h prior to the 20 h data collection period. Evaluation of spectra derived from the start and end of the 20 h collection block showed no evidence for evolution of either spectral parameters or component areas. Furthermore, spectra of freshly mounted samples taken directly to an elevated temperature and equilibrated for 3 h were found to be indistinguishable from those obtained from samples that had been raised to the same temperature in a series of steps spanning 7−10 days. We therefore conclude that the spectra presented here represent the equilibrium state of these materials, at least on a time scale of several days.

Results and Discussion

Samples of $LiFePO_4$ were prepared from either Fe(II) or Fe(III) precursors and oxidized using $NOBF_4$ to give the target stoichiometries, Li_xFePO_4 ($x = 0 \rightarrow 0.75$). The room-temperature Mössbauer spectra of the two parent compositions, $LiFePO_4$ and $FePO_4$, along with the two-phase mixtures corresponding to the stoichiometries: $Li_{0.75}FePO_4$, $Li_{0.55}FePO_4$, and $Li_{0.25}FePO_4$, are displayed in Figure 1. The contributions of the localized, static Fe^{2+} and Fe^{3+} components in the two-phase mixtures are readily apparent. They are characterized by two doublets with Mössbauer parameters of IS = 1.2 mm/s, QS = 3.0 mm/s and IS = 0.42 mm/s, QS = 1.5 mm/s, typical of Fe^{2+} and Fe^{3+} in these materials, respectively, which have been well characterized by this technique.[4] The relative areas of the two components can be used to confirm that the target starting stoichiometries were achieved by oxidation because the Li content, x, is related to the areas of the Fe^{2+} and Fe^{3+} components through:

$$x = A_{Fe}{}^{2+}/(A_{Fe}{}^{2+} + A_{Fe}{}^{3+})$$

where $A_{Fe}{}^{2+}$ and $A_{Fe}{}^{3+}$ are the areas of the two phases in the Mössbauer spectrum. Typical line widths (half-width at half-maximum) at 300 K for the Fe^{2+} and Fe^{3+} components were 0.150(2) and 0.154(1) mm/s, respectively, significantly above our instrumental limit of 0.113 mm/s. The samples typically contained about 5% of impurity phases, which are apparent in the spectra shown in Figure 1 as additional lines. Examples include the line at +0.8 mm/s due to an Fe^{3+} impurity in the $x = 1$ pattern and at +2.7 mm/s in the $x = 0$ pattern due to an Fe^{2+} impurity. The contributions of these impurity phases were included in all of the fits presented here.

Mössbauer spectra recorded at temperatures above 400 and up to 700 K nicely illustrate the evolution from the initial two-phase composition to the solid solutions $Li_xFe^{2+/3+}PO_4$ as a function of temperature (Figure 2). For each temperature point, a 3 h thermalisation time was employed followed by a counting time of 20 h, giving an overall time of 1 day per temperature point. Thus, each experiment in the temperature range between 400 and 700 K was recorded over the period of about 11 days. The time period was chosen on the basis of XRD studies of solid solution behavior in this system that utilized a 12 h heating period to achieve "quasi-equilibrium" at any selected temperature.[22] At 650 K, they reported that equilibrium is reached rapidly within 30 min, but below 500 K, the kinetics are more sluggish. Even in this regime, however, very little change is observed between 12 h and 3−4 days. We also can be confident that close-to-equilibrium conditions were established in our case because monitoring of the Mössbauer spectra for longer periods of time for one representative sample ($Li_{0.55}FePO_4$; 48 h counting time) showed that no further significant changes occurred. Owing to the time required for each experiment, data were collected only on heating, not cooling where very sluggish kinetics dominate, along with the formation of secondary phases that could complicate the spectra. In Figure 2, we see that on heating the sample to 425 K, the spectrum of each sample is dominated by the contributions of the parent phases. By 500

(22) Dodd, J. L.; Yazami, R.; Fultz, B. *Electrochem. Solid-State Lett.* **2006** *9*, 131.

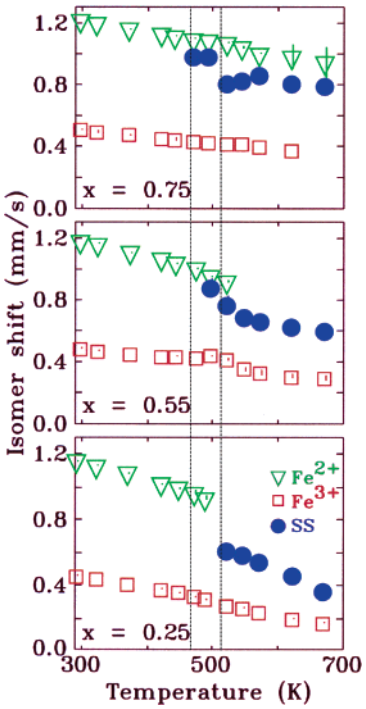

Figure 3. Change in isomer shift of the Fe^{2+}, Fe^{3+}, and the solid solution phases as a function of temperature for $Li_{0.25}FePO_4$, $Li_{0.55}FePO_4$, and $Li_{0.75}FePO_4$, demonstrating that the isomer shift of the solid solution phase lies between those of the Fe^{2+} and Fe^{3+} phases in all cases. The dotted lines represent the range of the transition temperature.

K, a new phase is visible that increases in fraction along with diminution of the parent phases on further heating. By 670 K, transformation to the single phase regime is essentially complete and the corresponding spectra are now dominated by one doublet.

The quantitative changes in the spectra on heating are more clearly seen by examining the temperature dependence of the fitted parameters. Figure 3 shows the variation in the isomer shift (δ) of the Fe^{2+} and Fe^{3+} components along with that of the solid solutions. It is clear that δ for the Fe^{2+} component is more strongly temperature dependent than for the Fe^{3+} component, and we found that this difference in temperature dependence is also seen in the spectra of the parent phases. Two important findings are evident from the plot. First, the transition temperature to the solid solution regime is about 495 K, in good accord with that found by XRD measurements that place it about 473−493 K.[18,22] The range in the transition temperature indicated by the dotted lines in the figure is discussed below. Second, the most striking feature of the solid solution phase is that in every case, its isomer shift (δ_{SS}) lies between that of the parent Fe^{2+} and Fe^{3+} phases. This shows that the iron valence is intermediate between 2+ and 3+. Furthermore, the average oxidation state of the starting two-phase $x(LiFePO_4)/y(FePO_4)$ mixture (where x and y are the relative ratios of the two components) dictates the precise value of the solid solution isomer shift. As the balance between Fe^{2+} and Fe^{3+} phases shifts toward Fe^{3+}, the average valence of the solid solution phase increases, and this is reflected in the lower δ_{SS}. Similar valence averaging has been reported in CoO and NiO at high temperatures.[23] The presence of this mixed iron Fe^{2+}/Fe^{3+} valence

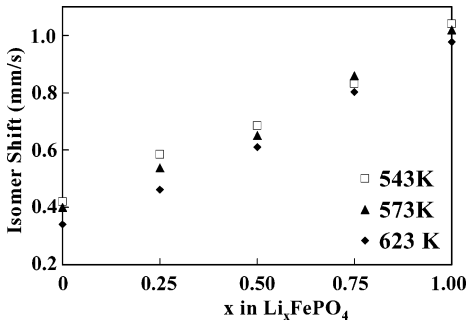

Figure 4. Plot of isomer shift vs x in Li_xFePO_4.

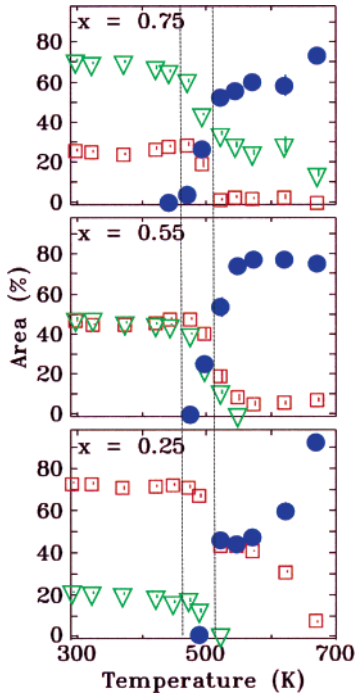

Figure 5. The relative areas of the Fe^{2+}, Fe^{3+}, and the solid solution phase as a function of temperature for $Li_{0.75}FePO_4$, $Li_{0.55}FePO_4$, and $Li_{0.25}FePO_4$. The Fe^{2+} and Fe^{3+} components disappear as the solid solution phase forms, first appearing at 500 K in all three samples. Note that the Fe^{2+} is consumed first. Symbols used correspond with those used in Figure 3.

state, expected for a stoichiometry Li_xFePO_4, was inferred from static bond-sum data, which showed averaged Fe−O bond lengths between the two oxidation states.[24] Here, however, we can pinpoint the exact temperature of the phase transition by the appearance of the solid solution signal in the Mössbauer spectra. This is valid even if kinetic delay initially gives rise to short coherence lengths within the crystal invisible to diffraction but visible to Mössbauer because is a local atomic probe.

Moreover, the isomer shift of the solid solution phase at any specific temperature increases *linearly* with increasing Li content (Figure 4), in accord with the decrease in the mean valence. This reveals the development of rapid electron hopping in the solid solution phase that averages the valence states on the time scale of the Mössbauer window. The temperature at which the parent phases are replaced by the SS phase is clearly delineated in a plot of the relative phase fractions as a function of temperature, shown in Figure 5. The areas effectively represent the close-to-equilibrium state of the samples as described above.

(23) Song, C.-J., Mullen, J. G. *Phys. Rev. B: Condens. Matter Mater. Phys.* **1976**, *14*, 2761.

(24) Delacourt, C.; Rodríguez-Carvajal, J.; Schmitt, B.; Tarascon, J.-M.; Masquelier, C. *Solid State Sci.* **2005**, *7*, 1506.

The average onset temperature for appearance of the SS (495 K) is essentially the same as reported in XRD studies (475−495 K),[18,22] as mentioned above. The latter report the onset of the transformation of two-phase mixtures of $LiFePO_4/FePO_4$ into a solid solution Li_xFePO_4 as composition independent, however. Our Mössbauer studies show that the temperature varies slightly with Li composition and, hence, Fe^{2+}/Fe^{3+} content. At the highest Fe^{2+} stoichiometry ($Li_{0.75}FePO_4$), the onset of the signal is at 470 K, whereas at the highest Fe^{3+} content ($Li_{0.25}FePO_4$), it is delayed until 520 K (also apparent in Figure 4). This may reflect the difference in mobility between electron carriers that would predominate in the former case, *vs* hole carriers that would predominate in the latter. Diffraction, which is sensitive to changes in the lattice, would not be able to detect this effect. These curves also indicate that the solubility of the Fe^{3+} phase within the mixture is less than that of the Fe^{2+} phase. Except for the sample $Li_{0.75}FePO_4$ (Figure 5) where the Fe^{2+} component is the initial majority phase, the Fe^{2+} component is consumed first as the temperature increases. The Fe^{3+} phase persists to high temperature in $Li_{0.55}FePO_4$ and $Li_{0.25}FePO_4$ even in the presence of substantial fractions of the SS phase. This suggests that there is a bias in solubility of the two phases in favor of Fe^{2+} dissolution. The persistence of some unconsumed majority phase in $Li_{0.75}FePO_4$ and $Li_{0.25}FePO_4$ probably reflects the presence of isolated regions that are unable to react. Alternatively, during preparation of the samples, oxidation of $LiFePO_4$ may proceed to completion in some very small crystallites to give particles composed entirely of $FePO_4$, which are then unable to form an SS phase.

That the materials show an average onset of rapid electron hopping behavior in the Mossbauer at *effectively the same* temperature as that reported from diffraction studies is highly significant. XRD studies showed that for compositions Li_xFePO_4 ($x = 0.04 \rightarrow 0.85$), the patterns for the two parent phases merge into one single phase that displays intermediate lattice parameters.[18,22] Neutron diffraction studies subsequently revealed that the lithium ions are fully disordered in the solid solution, which characterizes it as a single phase from a structural point of view.[24] The Mössbauer data allow us to go further in interpretation of the nature of the solid solution. If the randomizing of the lithium siting simply led to a *static* random distribution of the Fe^{2+} and Fe^{3+} within the lattice, then the Mössbauer spectrum would not change on entering the solid solution phase. However, the electrons are clearly dynamically delocalized on the Mössbauer time scale, and it is this behavior that is correlated with the random lithium population within the SS lattice. The question is whether averaging of the iron oxidation state drives the disorder of the Li^+ or vice versa. We believe it it is the former. We base this on previous observations of complex phase transitions that occur upon lithium de/intercalation in $Li_{3-x}V_2(PO_4)_3$ on a *static* scale, where Li-site ordering and electron ordering are coupled.[25,26] On charge, extraction of Li from $Li_2V_2(PO_4)_3$, which has an ordered $V^{3+/4+}$ valence state, occurs by a series of two-phase transitions to form $V_2(PO_4)_3$. However, the $V_2(PO_4)_3$ that is formed exhibits a disordered $V^{4+/5+}$ valence state. Insertion of Li into this lattice leads to solid solution behavior over a wide range. Thus two compositions $LiV_2(PO_4)_3$ can be obtained, one with ordered Li^+ (and ordered e^-); and the other with disordered Li^+ (and disordered e^-). Disorder of the mixed V^{4+}/V^{5+} state in $V_2(PO_4)_3$ formed on emptying of the lattice drives formation of the lithium SS on reinsertion.[25] For both the iron and vanadium cases, structural lattice effects that arise from bond-length changes in the framework when the valence state is averaged may result in the Li^+ disordered state being more thermodynamically stable.

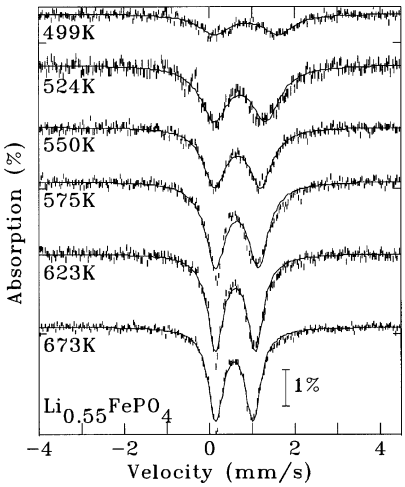

Figure 6. Mössbauer spectra of the $Li_{0.55}FePO_4$ phase recorded from 500 to 673 K, clearly showing the growth of the solid solution phase and the decrease in line width as motional narrowing sets in. These patterns were obtained by subtracting all other components from the spectra to illustrate the changes in the form of the solid solution spectra.

Analysis of the Mössbauer spectral evolution in the SS phases as a function of temperature can yield even more important information on the electron hopping rate owing to the time scale over which the dynamic process can be observed. Namely, for very slow fluctuations ($\tau_R \gg \tau_Q$; or events occurring on a time scale slower than the Mössbauer window of $\sim 10^{-6}$ s), a static pattern with sharp spectral features is obtained with no information on the dynamics.[21] As τ_R approaches τ_Q from above, a complex pattern develops with both the original static patterns coexisting with a severely broadened dynamic spectrum. Decreasing τ_R below τ_Q takes us into the motional narrowing regime and eventually a sharp, dynamically averaged pattern is regained. Figure 6 shows the motional narrowing of the solid solution sub-spectrum on heating the $Li_{0.55}FePO_4$ phase that is representative of all of the samples. At each temperature, the full spectrum was fitted using both parent phases, any impurity phase and also the solid solution phase. For illustrative purposes only, all contributions except that of the solid solution were then subtracted from the data to yield the patterns shown in Figure 6. Two changes are readily apparent: (i) the area of the solid solution phase grows rapidly on heating, and (ii) the spectral lines become progressively sharper as motional narrowing occurs. This latter change indicates that the small polaron transport becomes more rapid over the temperature window in which the Mössbauer experiment can "sense" the electron mobility; at temperatures lower than 500 K, the onset of electron mobility is just starting, whereas above 673 K, the mobility is too fast for the Mössbauer experiment to probe. Detailed analysis of the line width yields an electron hopping rate, and the temperature dependence of the line width allows us to extract an intrinsic activation energy for the small polaron hopping.

(25) Yin, S.-C.; Grondey, H.; Strobel, P.; Anne, M.; Nazar, L. F. *J. Am. Chem. Soc.* **2003**, *125*, 10402.
(26) Yin, S.-C.; Grondey, H.; Strobel, P.; Anne, M.; Nazar, L. F. *J. Am. Chem. Soc.* **2003**, *125*, 327.

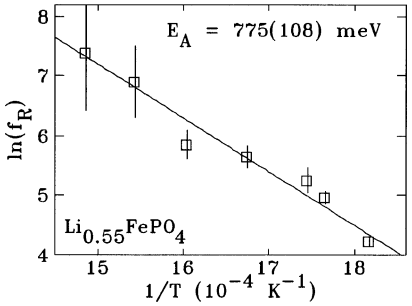

Figure 7. Plot illustrating the fit of the data for $\ln(1/\tau_F)$ vs. $1/T$ from which the activation energy, E_a, of 775 ± 108 meV for the motional narrowing process was derived.

Fitting of the patterns in Figure 6 shows that the lines are well approximated by Lorentzian line shapes, consistent with dynamic effects rather than static disorder being the primary source of the line broadening. Furthermore, the observed sharpening of the lines is more consistent with motional narrowing, which might be expected on heating, than with a reduction in disorder effects. These observations, confirmed by the relaxation times derived below, suggest that the dynamics being observed are in the motional narrowing limit ($\tau_R \leq \tau_Q$), which allows us to greatly simplify our analysis. Treating the observed line width as the sum of the phase line width, Γ_T, which includes all static contributions (resolution limitations, chemical disorder, etc.) and a dynamic contribution, Γ_R, we can separate and track the temperature dependence of the dynamic line broadening.[21,27] The only free parameter is the choice of Γ_T, the phase line width. None of the components in any of the spectra gave line widths close to our instrumental resolution of 0.113 mm/s, and thermal stability of the samples limited our upper working temperature so that we could not be certain of having achieved a fully motionally narrowed state. We therefore took the observed line width at our maximum temperature (0.212(7) mm/s) as an upper limit on Γ_T and adjusted the value downward slightly so as to obtain the best scaling on an Arrhenius plot. This led to a final choice of $\Gamma_T = 0.205$ mm/s for the data in Figure 6 for $Li_{0.55}FePO_4$. Most of our quoted uncertainty in E_a derives from the uncertainty in our choice for Γ_T; however, as shown below, our data span a factor of 40 in time scales, giving us reasonable coverage of the dynamics.

With all of the parameters determined,[27] we can extract $\Gamma_T(T)$ and hence $\tau_F(T)$. Assuming conventional Arrhenius activated dynamics, we fit the data for $\ln(1/\tau_F)$ vs. $1/T$ to derive an activation energy, E_a, of 775 ± 108 meV for the motional narrowing process (Figure 7). It is interesting to compare this E_a with values derived from other measurements. Dc conductivity provides estimates of between 390 and 500 meV, but the latter are not a true estimate of carrier activation energy in the lattice. Measurements performed on pressed powders of $LiFePO_4$ are strongly affected by the conductive carbon or other impurities present at the grain boundaries.[28] The most reliable value in our opinion is from ac impedance spectroscopy, of about 630 meV.[11] In principle, this technique could allow one to distinguish between grain boundary and inherent bulk contributions, but in practice, this can be fraught with uncertainty. The challenge in reliably fitting equivalent resistance circuits can lead to widely ranging numbers, for example, as low as 155 meV for the same measurement.[12]

Scheme 2. Schematic Illustrating Small Polaron Hopping within the Corner-Shared FeO_6 Octahedra Spanning the *bc* Plane of the Olivine Lattice

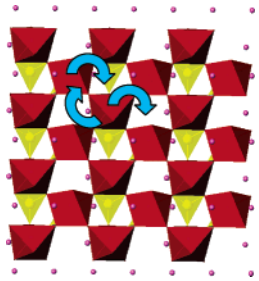

In contrast, Mössbauer gives a microscopic measure of the intrinsic barrier to transport within the lattice. Considering the uncertainty in selecting Γ_T, our one-σ lower bound (670 meV) is remarkably close to the ac conductivity result cited above. Not surprisingly, our measured E_a of 775 ± 108 meV is higher than that estimated by first-principle pseudopotential calculations of the "free" small polaron activation energy in $LiFePO_4$ (215 meV) or $FePO_4$ (175 meV).[13] It is important to note that strong binding of the polaron to the lithium-ion (calculated to be ~370−500 meV by the same authors) will raise the activation energy substantially. Inclusion of this contribution to the free polaron E_a for $LiFePO_4$ raised the overall activation energy to a value of 585−715 meV, similar to that measured experimentally, and fully consistent with our result for E_a. Strong interaction is inherent in our proposed correlated hopping of the ion and electron carriers described above. That our E_a is so much higher than that predicted for unconstrained polaron migration lends our model strong support. It further indicates that the transport is limited by neither carrier alone, but by their *concerted diffusion* through the lattice. Thus, the activation energy for free polaron mobility is raised by strong interaction with the lithium ion, and the converse is also true: the activation energy for lithium ion transport is higher than predicted in the absence of coupling to the localized electrons.

The small polaron carrier mobility is expected to be two-dimensional. This is depicted in Scheme 2, which shows the connectivity within the (100) plane of the $LiFePO_4$ (*Pnma*) lattice. Transport perpendicular to the plane would have an very high activation energy because the FeO_6 octahedra are not directly connected along this direction but are spanned by intervening PO_4^{3-} units. It is therefore possible to loosely estimate an "electron diffusion coefficient" from the standard diffusion relationship: $D = \lambda^2/\nu$, where λ = path length and ν is the frequency of the hop. The approximation neglects two additional contributions, the first being the geometrical term that takes into account the nature of the diffusion path. For an essentially square lattice presented by the *bc* plane, this factor is close to one even though the diffusion is constrained by the

(27) In our assumed limit, where two Mössbauer lines at $\omega_0 + \Delta\omega$ and $\omega_0 - \Delta\omega$ collapse to a single line at ω_0, the Mössbauer spectrum $\Phi(\omega)$ takes the form (reference 16): $\phi(\omega) = \text{const}/\{\Gamma_T - i(\omega - \omega_0) + [(\Delta\omega^2)/\omega_R]\}$ and Γ_R is given by $(\Delta\omega^2)/\omega_R$. Strictly speaking, we have two doublets from Fe^{2+} and Fe^{3+} that collapse to form the solid solution doublet, so that each side of the final doublet is formed from one line from each of the Fe^{2+} and Fe^{3+} components. Here, we treat each half of the problem as independent and identical because there are no apparent asymmetries in the solid solution spectrum. We estimate $\Delta\omega$, the gap between the component lines, at about 1 mm/s. This choice impacts the absolute values of the relaxation rates derived from our analysis but does not affect the derived activation energy, which is the focus of this analysis.

(28) Herle, P. S.; Ellis, B.; Nazar, L. F. *Nat. Mater.* **2004**, *3*, 147.

connectivity of the FeO_6 octahedra[10,29] The correlation term is a measure of the success probability of the hop, and can vary from 1 to 10^{-3}.[10,30] We assume this value is one in our "back-of-the-envelope" calculation, because a process whereby the electron or hole carrier hopped back to the original site would be too fast to show up on the Mössbauer time scale (the Mössbauer spectrum is only affected by successful hop events). Therefore, based on the hop distance (average = 3.67Å) and the hop frequency (10^8 sec^{-1}) from the time scale of the Mössbauer window, we estimate a value of $D \approx 10^{-7}$ cm^2/sec. Even though this may be off by an 1 or 2 orders of magnitude, it is noteworthy, perhaps coincidental, that it is within the range calculated for the lithium diffusion coefficient in the absence of interaction with electron carriers, of between 10^{-7} and 10^{-9} cm^2/sec.

With the above considerations in mind, the fact that the phase transition to the SS in Li_xFePO_4 is driven by an increase in temperature can be explained in simple terms. For an electron to move to an adjacent Fe^{III} site from an Fe^{II} site, the Franck−Condon principle dictates that the iron nuclei must first assume a configuration that brings their two electronic energy levels into coincidence: a process accompanied by thermal fluctuations in the lattice. This can also be described by Marcus theory, which establishes that electron transfer between two redox sites takes place only after metal−ligand bond lengths have been altered enough to allow the transfer to occur adiabatically (i.e., without further change in energy).[31]

(29) Van der Ven, A.; Ceder, G.; Asta, M.; Tepesch, P. D. *Phys. Rev. B: Condens. Matter Mater. Phys.* **2001**, *64*, 184307.
(30) Austin, I. G.; Mott, N. F. *Science* **1970**, *168*, 3297.
(31) Marcus, R. A. *Pure Appl. Chem.* **1977**, *69*, 13.

Conclusions

The Mössbauer experiments pinpoint the temperature of formation of the solid solution on heating $LiFePO_4/FePO_4$ above 500 K and clearly show that small polaron transport is reponsible for electron transport. The isomer shift of the averaged $Fe^{2+/3+}$ environment is directly related to the averaged oxidation state in $Li_{1-x}FePO_4$. The onset of rapid small polaron hopping on the time scale is precisely correlated with the temperature that the lithium ions begin to disorder in the lattice, showing that the two events are correlated. Furthermore, we suggest that the coupled lithium/electron transport is also coupled to vibrational (phonon) modes in the phosphate lattice that are accessed at elevated temperature. In this excited state, the Fe−O bond lengths in the $Fe^{II}O_6$ and $Fe^{III}O_6$ sites become transiently equivalent, permitting the electron hops to occur in a concerted manner that spans a large lattice domain. Because this is based on small polaron transport, the process is controlled by the activation energy, which remains invariant. However, the carrier density can be modified, and this has important ramifications for electrode material design. The exact nature of the process underlying the activation and electron−ion coupling energy in Li_xFePO_4 will arise from investigation of the phonon spectrum. Experiments along these lines are currently underway and should lead to further understanding of electron transport and mixed conduction processes in these important materials.

Acknowledgment. We thank Dane Morgan (University of Wisconsin) for useful discussions and Gerbrand Ceder (MIT) for a copy of their paper prior to publication.

JA0614114